JOURNAL OF CATALYSIS 53, 208–227 (1978)

The Selective Oxidation of CH_3OH to H_2CO on a Copper(110) Catalyst

ISRAEL E. WACHS[1] AND ROBERT J. MADIX

Department of Chemical Engineering, Stanford University, Stanford, California 94305

Received August 22, 1977; revised December 12, 1977

The oxidation of methanol to formaldehyde was studied on a Cu(110) single crystal by flash decomposition spectroscopy. The Cu(110) surface was preoxidized with oxygen-18; deuterated methanol, CH_3OD, was used to distinguish the hydroxyl hydrogen from the methyl hydrogens. Very little methanol chemisorbed on the oxygen-free Cu(110) surface, but the ability of the copper surface to chemisorb methanol was greatly enhanced by surface oxygen. This enhancement was absent subsequent to reduction of the surface by methanol itself. CH_3OD was selectively oxidized upon adsorption at 180°K to adsorbed CH_3O and $D_2{}^{18}O$. The methoxide was the most abundant surface intermediate and decomposed at about 365°K to formaldehyde and hydrogen with a first-order rate constant equal to $5.2 \pm 1.6 \times 10^{12} \exp(-22.1 \pm 0.1\ \text{kcal/mole}/RT)\ s^{-1}$. To a lesser extent some methanol was oxidized to $HC^{16}O^{18}O$ which subsequently decomposed to $C^{16}O^{18}O$ and hydrogen with a first-order rate constant equal to $8 \pm 2 \times 10^{13} \exp(-30.9 \pm 0.2\ \text{kcal/mole}/RT)\ s^{-1}$. A pronounced maximum in oxidation activity with surface oxygen coverage was observed.

1. INTRODUCTION

The oxidation of methanol to formaldehyde is a very important industrial process that was discovered more than a century ago, but the mechanism of oxidation and the function of oxygen in this process are still not completely understood (*1*). The commercial oxidation of methanol is presently performed with two types of catalysts (*2*). The first or classical procedure uses a copper or silver catalyst in the form of gauze or pellets at temperatures between 600 and 725°C. A rich mixture of methanol with air is employed. The second method uses an oxide catalyst near 350°C, such as iron-molybdenum oxide, and employs a lean mixture of methanol in air to produce formaldehyde that is substantially free of unreacted methanol. The gases resulting from the first process contain 18 to 20% hydrogen and less than 1% oxygen while the gases resulting from the oxide process contain unreacted oxygen and no appreciable concentration of hydrogen. The other major by-product is carbon dioxide, and trace amounts of CO, HCOOH, CH_4, and $H_2C(OCH_3)_2$ are also formed.

The industrial oxidation of methanol to formaldehyde was first believed to be a gas-phase oxidation process (*2, 3*):

$$CH_3OH + \tfrac{1}{2}O_2 \rightarrow H_2CO + H_2O. \quad (1)$$

The above mechanism was thought to occur between an oxygen atom adsorbed on the catalyst and methanol from the gas phase. This is still believed to be the oxidation mechanism when an oxide catalyst is employed. However, mechanistic studies of the metal-catalyzed process led subsequent investigators (*4*) to suggest that, overall, the reaction was either a dehydrogenation step, followed by the oxidation of hydrogen until all of the oxygen in the gaseous

---

[1] Present address: Corporate Research Laboratories, Exxon Research and Engineering Company, Linden, N.J. 07036.

0021-9517/78/0532-0208$02.00/0

mixture was consumed,

$$CH_3OH \rightleftarrows H_2CO + H_2, \qquad (2)$$

$$H_2 + \tfrac{1}{2}O_2 \rightleftarrows H_2O, \qquad (3)$$

or a combination of the dehydrogenation and oxidation reactions, steps (1) to (3). Consequently, early work on this reaction suggested the functions of oxygen to be (*5*): (a) to displace the dehydrogenation equilibrium to the right; (b) to keep the catalyst "active," and (c) to supply heat to make the process self-sustaining since the oxidation reactions, steps (1) and (3), are exothermic.

The importance of oxygen in this reaction was carefully investigated by Lawson and Thomson (*6*) to determine its influence on the activity of copper toward methanol decomposition. These results revealed that copper powders, *prepared by reduction of copper oxide with hydrogen,* catalyzed the decomposition of methanol, but were eventually poisoned or deactivated. When oxidized copper films were partially reduced by hydrogen, a decrease in the extent of methanol decomposition was noted. Bulk copper metal, in the form of wire or foil, was not active toward the decomposition of methanol. The copper foils and wires could be activated by oxygen treatments at elevated temperatures. It was concluded that *oxygen must be present in the copper for it to be active.* Other investigators also reported that the activity of their copper catalysts were not maintained, and it was always necessary to reactivate their catalysts by exposure to oxygen (*7–11*).

The present study was motivated by the lack of information available about the oxidation of methanol to formaldehyde on a *molecular level.* The oxidation of methanol was studied on a Cu(110)-oriented single crystal under ultrahigh vacuum conditions with the modern tools of surface science. The purpose of this work was (i) to investigate the mechanism and kinetics of the oxidation of methanol to formaldehyde and (ii) to determine the function of oxygen in this reaction.

2. EXPERIMENTAL

The flash desorption experiments were conducted in the stainless steel ultrahigh vacuum (UHV) system previously described (*12*). The UHV chamber was equipped with a PHI four-grid LEED-Auger optics, an argon ion bombardment gun, and a UTI-100C quadrupole mass spectrometer. The (110)-oriented copper single-crystal sample was heated from the rear by radiation from a tungsten filament. Except where noted, a heating rate of 4 to 5°K s^{-1} was employed. The sample could be cooled to about −95°C by heat conduction through a copper braid attached to a liquid nitrogen-cooled copper tube. The methanol was introduced onto the copper surface through a stainless steel dosing syringe directed at the front face of the crystal. The mass spectrometer signal for each product produced during the flash desorption was directly proportional to the desorption rate because of the high pumping speed of the system.

High-purity CH_3OH (99.9 mole%) was purchased from Fischer Scientific Co. and was purified by prolonged pumping at −84°C until a constant vapor pressure of 25 μm was obtained. The final vapor pressures of the methanol samples were in good agreement with the tabulated vapor pressure reported in the literature (*13*). Deuterated methanol, CH_3OD (99 atom% D), was obtained from ICN Life Sciences and was similarly purified. NMR analysis of the CH_3OD sample verified that only the hydroxyl hydrogen was deuterated. The only function of the pumping step was to outgas air from the samples. The alcohol vapor obtained above liquid CH_3OD at −84°C was used directly for the adsorption studies on copper.

Surface cleanliness was achieved at the beginning of each experiment by argon ion sputtering and was verified by Auger electron spectroscopy (AES). In previous studies on Ni(110) the AES calibrations for a surface carbon monolayer (*12*) and a surface oxygen monolayer (*14*) were obtained. Since the Auger sensitivities for copper and nickel are almost identical, the Ni(110) calibration standards for a surface monolayer of oxygen and carbon were also applied to the Cu(110) surface after correcting for the slightly different Cu and Ni sensitivities (*15*). AES analysis subsequent to the flash decomposition of methanol from a partially oxidized Cu(110) surface revealed the presence of surface carbon and oxygen. Oxygen did not desorb from the Cu(110) surface at the coverages used in this study when the sample was heated to 450°C, but excess oxygen was readily removed by exposing the sample to methanol for 100 s and flashing to 275°C. This procedure reproducibly formed an oxygen-free surface at the end of each flash and prevented the accumulation of oxygen on the copper surface. Auger analysis at the end of the day revealed the presence of 15 ± 3% of a surface carbon monolayer; surface carbon when present did not exhibit the characteristic Auger fine structure of surface carbide or surface graphite (*16*) and may have been amorphous carbon. This amount of surface carbon did not influence the reactions investigated because the first flash decomposition spectrum of the day was always reproduced at the end of the day.

Enriched oxygen (99% $^{18}O_2$) was purchased from Bio-Rad Laboratories and was introduced into the background of the UHV chamber through a variable leak valve. An oxygen background pressure of 1×10^{-8} Torr was always maintained throughout the adsorption of oxygen, and only the exposure time was varied; the copper sample was kept at 22 ± 10°C during the adsorption of oxygen. The oxygen exposure was varied from 0 to 10 Langmuirs (a Langmuir is defined as 1×10^{-6} Torr-s of oxygen exposure); the surface coverages of oxygen were determined by AES for several different oxygen exposures and are tabulated in Table 1. An initial sticking probability of ~5 $\times 10^{-2}$ for oxygen on the Cu(110) surface was calculated from the initial slope of the data in Table 1. No other values for the sticking probability of oxygen surfaces are available for comparison.

TABLE 1

Surface Coverages of Oxygen as Determined by AES[a]

Oxygen exposure (Langmuirs)	Surface coverage of oxygen (fraction of monolayer)
0.2	0.04
0.45	0.05
1.2	0.14
2.0	0.22
5.0	0.40

[a] Calibration standards for a surface monolayer of oxygen and carbon were obtained from the Ni(110) surface and corrected for the different Auger sensitivities of Cu(110) and Ni(110).

The products observed in this study were identified by carefully comparing their observed cracking patterns in the mass spectrometer with those tabulated in the literature. Once the product was identified, the ionized parent molecule, i.e., $m/e = 33$ for CH_3OD, $m/e = 30$ for H_2CO, etc., was used to monitor the product. The only exception was CH_3OH for which $m/e = 31$ was monitored in order to avoid overlap with the CH_3OD $m/e = 32$ signal. A more extensive discussion on product identification by mass spectrometry will be found in Appendix II.

3. RESULTS

A brief summary of the results is presented first to assist the reader. This summary is confined to the major observations, emphasizing their qualitative features.

Several reaction products were formed while heating the Cu(110) surface predosed

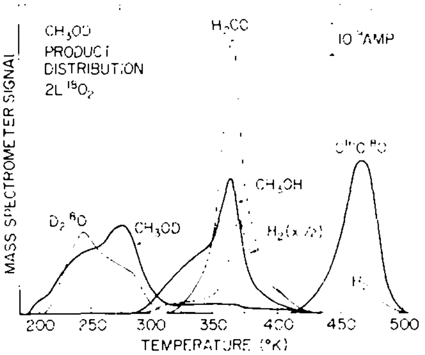

FIG. 1. Flash decomposition spectrum following CH_3OD adsorption at 180°K on a Cu(110) surface that was predosed with 2 Langmuirs of $^{18}O_2$ at 295 ± 10°K. The CH_3OD exposure was 100 s.

with $^{18}O_2$ on which CH_3OD was adsorbed. These products were $D_2{}^{18}O$, H_2CO, CH_3OH, H_2, and CO_2. Careful studies showed each of these products to be formed by first-order kinetics. $D_2{}^{18}O$ was evolved first as a result of the specific interaction between CH_3OD and $^{18}O_{(a)}$ to form $CH_3O_{(a)}$. This intermediate then decomposed to form H_2CO and H_2. The CO_2 was formed via an $HCOO_{(a)}$ intermediate which was more stable (though less predominant) than $CH_3O_{(a)}$.

There was an enhancement in the adsorption of CH_3OD and the amount of products formed by over an order of magnitude as the concentration of surface oxygen was increased. In effect, the surface oxygen acted as a promoter for both dissociative and nondissociative alcohol adsorption. The production of H_2CO exhibited a maximum as the surface oxygen concentration was increased. A more detailed presentation of the results now follows.

The product distribution subsequent to CH_3OD adsorption near 180°K on the copper surface predosed with 2 Langmuirs of $^{18}O_2$ is shown in Fig. 1. Below room temperature $D_2{}^{18}O$ and CH_3OD were the only species to desorb; $D_2{}^{18}O$ accounted for 75% of the water formed below room temperature; the remaining water was in the form of $HD^{18}O$ (10%) and $H_2{}^{18}O$ (15%). Slightly above room temperature H_2CO, CH_3OH, and H_2 evolved simultaneously indicating that they originated from the same surface intermediate.[1] The products H_2CO, CH_3OH, and H_2 had to

---

[1] The thermal programmed reaction product spectrum is a kinetic spectroscopy. Products that are emitted simultaneously therefore have the same rate as a function of temperature and must originate from the same mechanism. When the evolution of these products is first order, they originate from the same rate-determining intermediate.

TABLE 2

The Interaction of Simple Molecules with the Oxygen-Free Cu(110) Surface[a]

State	T_p (°K)	E (kcal/mole)	ν (s^{-1})	E^*[b] (kcal/mole)	Source
CO/CO	223	14	4×10^{13}	13.5	Ying (*17*)
CO/CO_2	223	14	4×10^{13}	13.5	This work
$H_2O(\alpha)/H_2O$	235	—	—	14.2	Ying (*17*)
$H_2O(\beta)/H_2O$	285	—	—	17.3	Ying (*17*)
C_2H_4/C_2H_4	224	—	—	13.5	This work
H_2CO/H_2CO	225	—	—	13.5	This work
D_2/D atoms	336	12 ± 1[c]	$10^{7\pm1}$[c,d]	—	This work
$H_2 + CO_2/HCOOH$	470	32 ± 1	$8 \pm 2 \times 10^{13}$	29.0	Ying (*17*)

[a] Adsorption was always done with the Cu(110) sample cooled to 180°K.

[b] E^* is the activation energy calculated for a single first-order rate-limiting step from T_p, assuming $\log_{10} \nu = 13$.

[c] The kinetic parameters were calculated by plotting $\ln(R/C^2)$ vs $1/T$.

[d] Second-order process and frequency factor has units of square centimeters per second.

result from the decomposition of a surface *intermediate* since otherwise they would have desorbed at lower surface temperatures, characteristic of their desorption (see Table 2). Above room temperature CH_3OH was formed even though CH_3OD was initially adsorbed on the copper surface. No HD or D_2 was observed to desorb throughout the entire temperature range because *all of the deuterium atoms released upon adsorption were involved in the formation of water.* At higher surface temperatures $C^{16}O^{18}O$, H_2, and $H_2{}^{18}O$ (not shown in Fig. 1) also evolved simultaneously near 470°K, suggesting that these species originated from another surface intermediate. $C^{16}O^{18}O$ accounted for 84% of the total carbon dioxide signal; the small amounts of $C^{16}O_2$ and $C^{18}O_2$ probably resulted from methanol that dissociated upon adsorption. No other flash decomposition products were observed; in particular, carbon monoxide, methane, methyl formate, methylal, dimethyl ether, and ethanol were absent from the spectrum.

The desorption properties of various simple gases from the oxygen-free Cu(110) single-crystal surface, subsequent to adsorption at ~180°K, are presented in Table 2. The notation $A(\alpha)/B$ refers to the α state or desorption peak for gas A following adsorption of gas B. The tabulated activation energies and preexponential factors were determined by heating rate variation (*18*) unless otherwise stated. E^* was calculated from the peak temperature of each state, assuming a first-order reaction step with a frequency factor $\nu = 10^{13}\ s^{-1}$ to provide a relative value for those states for which kinetic parameters were not available. Note that all the small molecules that exhibited first-order desorption kinetics (CO, H_2O, H_2CO, and C_2H_4) desorbed with peak temperatures between 223 and 285°K. Therefore all of the product peaks above 285°K were formed by surface reaction-limited processes.

a. CH_3OD and CH_3OH/Methanol

Methanol desorbed both as CH_3OD and as CH_3OH (see Fig. 1) subsequent to the adsorption of CH_3OD on the oxidized copper surface. The CH_3OD desorption peaks were only observed below 300°K and represented the desorption-limited evolution of methanol; the CH_3OH peaks were only observed above 300°K and were reaction limited. These results suggested that the CH_3OH peaks resulted from CH_3OD that had released its D atom upon adsorption to form CH_3O and subsequently reacted with a surface H atom to form CH_3OH.

The above results suggested the possibility of forming *CH_3OD above room temperature* by maintaining a sufficient concentration of D atoms on the copper surface above room temperature. Since D_2 does not stick on copper, but deuterium atoms have a high sticking probability, the ionizer of the mass spectrometer was used to dissociate D_2 to deuterium atoms. A D_2 background pressure of about 10^{-6} Torr was maintained during the flash decomposition with the front of the sample facing the mass spectrometer with an initial CH_3O coverage of 25% of a monolayer; the CH_3OD signal shown in Fig. 2 was moni-

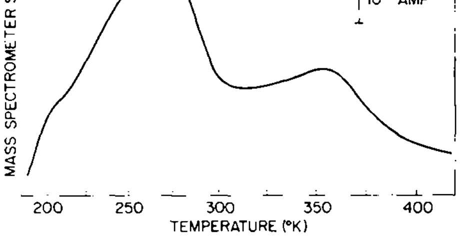

FIG. 2. The formation of CH_3OD from surface methoxide and background deuterium above 300°K following adsorption of CH_3OD at 180°K on a Cu(110) surface preoxidized with 2 Langmuirs of $^{18}O_2$ at 295 ± 10°K. The CH_3OD exposure was 100 s and the D_2 background pressure was $\sim 1 \times 10^{-6}$ Torr.

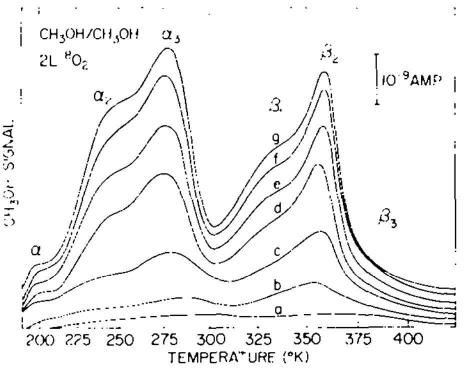

FIG. 3. The CH_3OH desorption spectrum subsequent to the adsorption of CH_3OH at 180°K on a Cu(110) surface predosed with 2 Langmuirs of $^{18}O_2$ at 295 ± 10°K. The CH_3OH exposures were (a) 1, (b) 5, (c) 13, (d) 27, (e) 50, (f) 75, and (g) 100 s.

tored during this experiment. Under these conditions *CH_3OD desorbed both above and below room temperature*. The CH_3OD peak above room temperature corresponded to that previously only recorded for CH_3OH. It was concluded from this experiment that the following reaction occurred at 350°K,

$$CH_3O_{(a)} + D_{(a)} \rightarrow CH_3OD_{(g)}, \quad (4)$$

and that methoxide, CH_3O, was a surface intermediate. A small amount of the CH_3OD could also have been formed by the Rideal-Ely mechanism, but under these experimental conditions the surface concentration of the deuterium atoms was very high, and the Langmuir-Hinshelwood mechanism was probably the preferred reaction pathway. This experiment demonstrated that the methanol peaks below 300°K were desorption limited and the methanol peaks above 300°K were reaction limited.

The CH_3OH/CH_3OH spectra from the copper surface predosed with 2 Langmuirs of $^{18}O_2$ exhibited multiple peaks above and below room temperature as shown in Fig. 3. Deuterated methanol, CH_3OD, was not utilized for this coverage variation study, but the above discussions demonstrated that only the methanol peaks below 300°K were desorption limited. The methanol desorption spectra below room temperature exhibited three peaks (α_1, α_2, and α_3). The desorption of $CH_3OH(\alpha_3)/CH_3OH$ was a first-order process as evidenced by the invariance of the peak position with methanol exposure. The overlap of the CH_3OH peaks prevented an accurate determination of their kinetic parameters. The methanol flash decomposition spectra above room temperature exhibited two major peaks (β_1 and β_2). A minor β_3 peak is not well defined in Fig. 3 and is more distinctly shown in Fig. 11. The $CH_3OH(\beta_2)/CH_3OH$ peak was the most prominent, and the constant peak temperature with increasing methanol exposure revealed that the rate-limiting step was a first-order surface process. This step was not desorption of the alcohol, and the above results showed that the second-order step (4) must have been fast under the conditions of this experiment. The rate-determining step was thus a first-order reaction preceding step (4). The $CH_3OH(\beta_2)/CH_3OH$ peak corresponded to that observed for $H_2CO(\beta_2)/CH_3OH$ and will be further discussed below in conjunction with formaldehyde formation.

b. H_2CO/Methanol

The formaldehyde flash decomposition spectrum is shown in Fig. 4 as a function of CH_3OH exposure. The formaldehyde spectra exhibited two peaks (β_2 and β_3). The $H_2CO(\beta_3)/CH_3OH$ state filled first and saturated at low exposures of methanol. The $H_2CO(\beta_2)/CH_3OH$ peak became predominant at higher exposures of methanol, and most of the formaldehyde desorbed from this state. The invariance of the β_2 peak with methanol exposure demonstrated that the surface reaction-limited step producing formaldehyde was a first-order process. The simultaneous production of $H_2CO(\beta_2)/CH_3OH$ and $CH_3OH(\beta_2)/CH_3OH$ revealed that both products originated from decomposition of the same

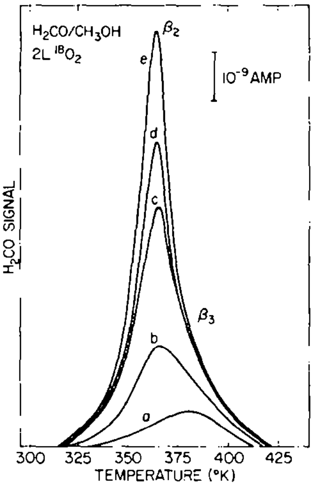

FIG. 4. The H_2CO flash decomposition spectrum as a function of CH_3OH exposure. The Cu(110) surface was always predosed with 2 Langmuirs of $^{18}O_2$ at 295 ± 10°K prior to the adsorption of CH_3OH at 180°K. The CH_3OH exposures were (a) 1, (b) 5, (c) 12, (d) 25, and (e) 50 s.

surface intermediate. It was concluded from these observations that formaldehyde was produced from the decomposition of the surface methoxide, CH_3O. The rate constant for $H_2CO(\beta_2)/CH_3OH$ was calculated by the method of heating rate variation to be

$$k_{H_2CO(\beta_2)/CH_3OH} = 5.2 \pm 1.6 \times 10^{12} \times \exp(-22.1 \pm 0.1\ \text{kcal/mole}/RT)\ \text{s}^{-1}. \quad (5)$$

The evolution of formaldehyde from this surface at ~365°K was not desorption limited and represented a reaction-limited step since H_2CO/H_2CO desorbed from Cu(110) at 225°K (see Table 2).

c. H_2/Methanol

The $H_2/^{18}O_2$, CH_3OH[2] spectra are shown, subsequent to the adsorption of CH_3OH on the copper surface exposed to 2 Langmuirs of $^{18}O_2$, as a function of methanol exposure in Fig. 5. Studies with deuterated methanol, CH_3OD, exhibited the same H_2 spectra, (see Fig. 1) indicating that these hydrogen peaks originated from the methyl hydrogens. The $H_2(\beta_2)/CH_3OH$ and $H_2(\beta_3)/CH_3OH$ peaks were very similar to the $H_2CO(\beta_2)/CH_3OH$ and $H_2CO(\beta_3)/CH_3OH$ peaks (see Fig. 4), but their peak maxima were several degrees higher. This suggested that both β-H_2 and H_2CO originated from the same surface intermediate, CH_3O, but that the hydrogen recombination process was not instantaneous near 370°K and the coverages utilized in this study. In addition, the activation energy determined for the $H_2(\beta_2)/CH_3OH$ peak was essentially identical to that previously calculated for $H_2CO(\beta_2)/CH_3OH$. This showed that, although the hydrogen recombination process delayed the H_2 peak by several degrees, it had only a minor influence on the determination of the activation energy for the production of the hydrogen atoms from the methoxide intermediate. Computer simulations of this series reaction process also verified these deductions. The origin of the $H_2(\beta_1)$ and $H_2(\gamma)$ peaks was different, however, as these additional peaks were absent from the formaldehyde spectrum, see Fig. 4. The $H_2(\beta_1)/CH_3OH$ peak tem-

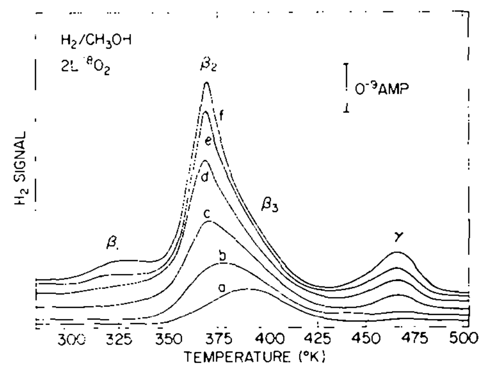

FIG. 5. H_2 desorption subsequent to CH_3OH decomposition on a partially oxidized Cu(110) surface. The Cu(110) surface was oxidized with 2 Langmuirs of $^{18}O_2$ at 295 ± 10°K prior to the adsorption of CH_3OH at 180°K. The CH_3OH exposures were (a) 1, (b) 5, (c) 12, (d) 25, (e) 50, and (f) 100 s.

---

[2] This notation indicates that $^{18}O_2$ was adsorbed prior to CH_3OH, and H_2 was then the observed product.

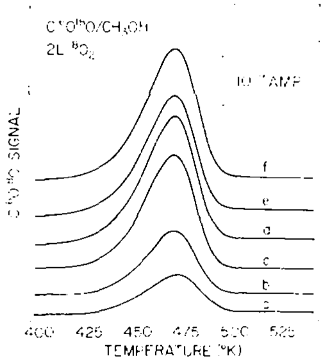

FIG. 6. The desorption of $C^{16}O^{18}O$ from the oxidation of CH_3OH on a Cu(110) surface predosed with 2 Langmuirs of $^{18}O_2$. The Cu(110) sample was oxidized at 295 ± 10°K and CH_3OH was adsorbed on the partially oxidized surface at 180°K. The CH_3OH exposures were (a) 2, (b) 8, (c) 25, (d) 50, (e) 100, and (f) 200 s.

perature corresponded to that of D_2/D_{atoms} (see Table 2) and was desorption limited. This desorbing hydrogen therefore originated from another surface intermediate which reacted below 325°K to produce surface hydrogen. Since the reaction $CH_3O_{(a)} + H_{(a)} \rightarrow CH_3OH$ should have been detectable above the highest desorption temperature of CH_3OH (300°K), it appears that the intermediate responsible for the $H_2(\beta_1)$ decomposed near 325°K. The $CH_3OD(\beta_1)/CH_3OD$ peak showed the same peak position as the $H_2(\beta_1)/CH_3OD$ which indicated that $CH_3O_{(a)}$ and $H_{(a)}$ reacted at 325°K. The simultaneous appearance of the H_2 and $C^{16}O^{18}O$ signals at 470°K will be discussed in greater detail below.

d. $C^{16}O^{18}O$/*Methanol*

The production of $C^{16}O^{18}O/CH_3OH$ was a first-order process as shown by the coverage variation study of Fig. 6 and the peak symmetry (*19*). The activation energy and the preexponential factor were calculated from heat rate variation studies and were determined to be

$$k_{C^{16}O^{18}O/CH_3OH} = 8.0 \pm 2.0 \times 10^{13} \times \exp(-30.9 \pm 0.2\ \text{kcal/mole}/RT)\ s^{-1}. \quad (6)$$

The $C^{16}O^{18}O$ peak position, activation energy, preexponential factor, and the ratio of $C^{16}O^{18}O/H_2(\gamma)$ were identical to the results obtained from the decomposition of HCOOH on this copper sample (see Table 2) in which it was found that HCOOH dissociatively adsorbed on the copper surface to yield formate, HCOO, and hydrogen atoms. The formate was very stable and dissociated at 470°K to produce CO_2 and H_2 simultaneously. In the present study oxygen-18 was still present on the copper surface at elevated temperatures, and a fraction of the hydrogen was oxidized to $H_2{}^{18}O$. The decomposition of the formate $HC^{16}O^{18}O$ was thus responsible for the simultaneous appearance of $C^{16}O^{18}O$, $H_2(\gamma)$, and $H_2{}^{18}O(\gamma)$ at 470°K. The production of $C^{16}O^{18}O$ evidently arose from the interaction of CH_3OH (or an intermediate therefrom) and the surface ^{18}O.

e. $H_2{}^{18}O$/*Methanol*

The $H_2{}^{18}O/CH_3OH$ spectra are presented in Fig. 7 as a function of CH_3OH exposure for a constant exposure of oxygen, 2 Langmuirs of $^{18}O_2$. Several $H_2{}^{18}O/CH_3OH$ peaks were observed: δ_1, δ_2, δ_3, and γ [the $H_2{}^{18}O(\gamma)/CH_3OH$ peak is not shown in Fig. 7]. The different water peaks were

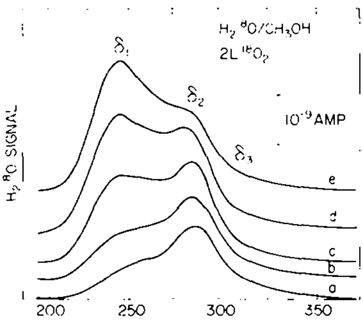

FIG. 7. The $H_2{}^{18}O$ desorption spectrum subsequent to the oxidation of CH_3OH on Cu(110). The CH_3OH was adsorbed at 180°K on a Cu(110) surface that was predosed with 2 Langmuirs of $^{18}O_2$ at 295 ± 10°K. The CH_3OH exposures were (a) 4, (b) 10, (c) 25, (d) 50, and (e) 100 s.

isolated by varying the methanol adsorption temperature, and the results are shown in Fig. 8. At low methanol exposures the δ_2 and δ_3 states filled first and saturated; at higher methanol exposures the δ_1 peak dominated the desorption of $H_2{}^{18}O/CH_3OH$. The desorption peaks exhibited first-order behavior since their peak maxima did not change with coverage. The $H_2{}^{18}O/CH_3OH$ spectra were identical to the desorption spectra of H_2O/H_2O from copper at low coverages (see Table 2). This information, coupled with the observations that (a) nearly all the water formed room temperature was deuterated when CH_3OD was used and (b) methoxide was a stable intermediate, suggested that methanol adsorbed dissociatively on the partially oxidized copper surface to form CH_3O and water with its hydroxyl hydrogen.

f. Oxygen Variation Studies

The oxygen exposure was varied from 0 to 10 Langmuirs while a constant methanol exposure of 100 s was maintained in order to examine the function of oxygen upon the oxidation of methanol on copper. The pronounced effect of the surface concentration of oxygen on the production of CH_3OH, H_2CO, and $C^{16}O^{18}O$ is shown in Fig. 9. Exposures of oxygen less than 2 Langmuirs enhanced the amount of CH_3OH, H_2CO, and $C^{16}O^{18}O$ observed, but exposures of oxygen greater than 2 Langmuirs decreased the yield of CH_3OH, H_2CO, and $C^{16}O^{18}O$. The formaldehyde production was very sensitive to the surface concentration of oxygen. The H_2CO signal increased over an order of magnitude between 0 and 2 Langmuirs of oxygen exposure. These results showed that the *sticking probability of methanol* on copper was very sensitive to the amount of oxygen on the surface; at low coverages of oxygen the sticking probability was enhanced, and at high oxygen coverages the sticking probability decreased. The detailed effects of surface oxygen on the rate of product production are presented in Appendix I. They are summarized briefly below.

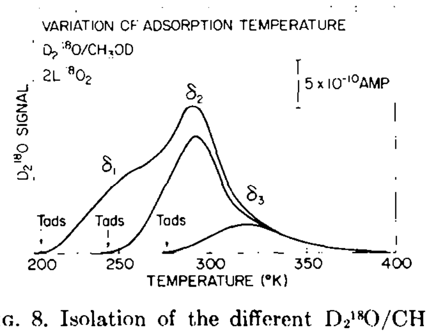

FIG. 8. Isolation of the different $D_2{}^{18}O/CH_3OD$ peaks by variation of the adsorption temperature. The CH_3OD exposure was 5 s and the Cu(110) surface was exposed to 2 Langmuirs of $^{18}O_2$ at 295 ± 10°K.

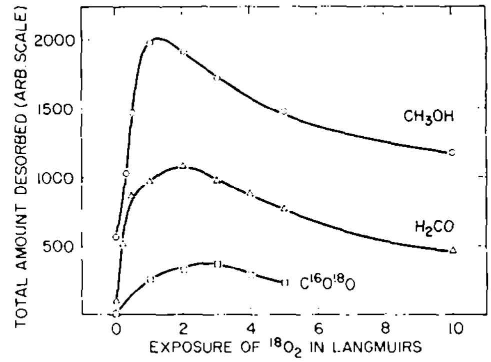

FIG. 9. The influence of oxygen exposure upon the production of CH_3OH, H_2CO, and $C^{16}O^{18}O$ following a 100-s exposure of CH_3OH at 180°K. The Cu(110) surface was always oxidized at 295 ± 10°K.

Very little methanol adsorbed on the surface free from the oxygen predose. To a minor extent the presence of surface oxygen altered the relative population of the methanol binding states and small shifts in peak temperatures were observed with increasing oxygen coverage. The binding energy of the $CH_3OH(\beta_2)/CH_3OH$ state increased by 1.5 kcal/gmole at the highest oxygen coverage. The reaction product peaks were affected substantially.

The fact that the amount of formaldehyde formed increased more than an order of magnitude at low oxygen exposure indicated that *it was necessary to have* *oxygen on the copper surface in order to produce efficiently H_2CO from CH_3OH.* This deduction was further supported by the observations that (i) predoses of $^{18}O_2$ on the surface of 1 to 3 Langmuirs *reduced* the sticking probabilities of CO and CO_2 (Appendix I) and (ii) CH_3OD interacted specifically with adsorbed ^{18}O to produce $D_2{}^{18}O$ and no D_2. The hydroxyl end of CH_3OD must have interacted specifically with the adsorbed oxygen during the dissociative adsorption of CH_3OD.

The results observed for the oxidation of CH_3OH on the copper(110) surface are tabulated below in Table 3. The kinetic parameters were calculated by the method of heating rate variation unless otherwise noted.

4. DISCUSSION

a. Mechanism and Kinetics

The results of the preceding section led to the following conclusions about the oxidation of CH_3OD on copper (110). (i) Surface oxygen enhanced the chemisorption of CH_3OD on the partially oxidized copper surface; (ii) CH_3OD interacted with surface oxygen through the hydroxyl end of the molecule during adsorption to form an adsorbed methoxide intermediate and water; (iii) H_2, H_2CO, and CH_3OH were formed from the reactions of a methoxide intermediate; (iv) the simultaneous appearance of H_2, $H_2{}^{18}O$, and $C^{16}O^{18}O$ at 470°K originated from the decomposition of $HC^{16}O^{18}O$; (v) the H_2 and CH_3OH peaks

TABLE 3

Oxidation of CH_3OH on Cu(110)[a]

State	T_p (°K)	E (kcal/mole)	ν (s^{-1})	E^{*b} (kcal/mole)
$CH_3OH(\alpha_1)/CH_3OH$	200 ± 5	—	—	12.1
$CH_3OH(\alpha_2)/CH_3OH$	245 ± 5	—	—	14.8
$CH_3OH(\alpha_3)/CH_3OH$	275	—	—	16.7
$CH_3OH(\beta_1)/CH_3OH$	330 ± 5	—	—	20.1
$CH_3OH(\beta_2)/CH_3OH$	365	—	—	22.4
$CH_3OH(\beta_3)/CH_3OH$	390	—	—	23.9
$H_2CO(\beta_2)/CH_3OH$	365	22.1 ± 0.1	$5.2 \pm 1.6 \times 10^{12}$	22.4
$H_2CO(\beta_3)/CH_3OH$	392	19.3 ± 0.4[c]	$1.5 \pm 0.7 \times 10^{10}$[c]	24.0
$H_2(\beta_1)/CH_3OH$	325 ± 5	—	—	19.8
$H_2(\beta_2)/CH_3OH$	370	22.0	3.6×10^{12}	22.6
$H_2(\beta_3)/CH_3OH$	390	—	—	23.9
$H_2(\gamma)/CH_3OH$	470	30.9 ± 0.2	$8.0 \pm 2.0 \times 10^{13}$	29.0
$C^{16}O^{18}O/CH_3OH$	470	30.9 ± 0.2	$8.0 \pm 2.0 \times 10^{13}$	29.0
$H_2{}^{18}O(\delta_1)/CH_3OH$	238	—	—	14.3
$H_2{}^{18}O(\delta_2)/CH_3OH$	290	—	—	17.6
$H_2{}^{18}O(\delta_3)/CH_3OH$	320	—	—	19.5
$H_2{}^{18}O(\gamma)/CH_3OH$	470	30.9 ± 0.2	$8.0 \pm 2.0 \times 10^{13}$	29.0

[a] The Cu(110) surface was oxidized at 295 ± 10°K and exposed to CH_3OH at 180°K.

[b] E^* is the activation energy calculated for a single first-order rate-limiting step from T_p, assuming $\log_{10} \nu = 13$.

[c] The kinetic parameters were calculated by plotting $\ln(R/C)$ vs $1/T$.

observed at 325°K resulted from the decomposition of an intermediate that was neither $CH_3O_{(a)}$ nor $HCOO_{(a)}$.

These observations suggested the following reaction scheme for the oxidation of CH_3OD on copper (110).

$$CH_3OD_{(g)} + {}^{18}O_{(a)} \rightarrow CH_3O_{(a)} + {}^{18}OD_{(a)} \tag{7a}$$

$$CH_3OD_{(g)} + {}^{18}OD_{(a)} \rightarrow CH_3O_{(a)} + D_2{}^{18}O_{(a)} \tag{7b}$$

$$CH_3O_{(a)} + {}^{18}O_{(a)} \rightarrow H_2C^{16}O^{18}O_{(a)} + H_{(a)} \tag{8}$$

$$H_{(a)} + {}^{18}OD_{(a)} \rightarrow HD^{18}O_{(a)} \tag{9}$$

$$2H_{(a)} + {}^{18}O_{(a)} \rightarrow H_2{}^{18}O_{(a)} \tag{10}$$

$$CH_3OD_{(g)} \rightarrow CH_3OD_{(a)} \tag{11}$$

$$D_2{}^{18}O_{(a)} \rightarrow D_2{}^{18}O_{(g)} \quad \{\delta_1, \delta_2, \delta_3\} \tag{12a}$$

$$HD^{18}O_{(a)} \rightarrow HD^{18}O_{(g)} \quad \{\delta_1, \delta_2, \delta_3\} \tag{12b}$$

$$H_2{}^{18}O_{(a)} \rightarrow H_2{}^{18}O_{(g)} \quad \{\delta_1, \delta_2, \delta_3\} \tag{12c}$$

$$CH_3OD_{(a)} \rightarrow CH_3OD_{(g)} \quad \{\alpha_1, \alpha_2, \alpha_3\} \tag{13}$$

$$\left.\begin{array}{ll} H_2C^{16}O^{18}O_{(a)} \rightarrow HC^{16}O^{18}O_{(a)} + H_{(a)} & (14) \\ H_{(a)} + H_{(a)} \rightarrow H_{2(g)} & (15) \\ H_{(a)} + CH_3O_{(a)} \rightarrow CH_3OH_{(g)} & (16) \end{array}\right\}\{\beta_1\}$$

$$CH_3O_{(a)} \rightarrow H_{(a)} + H_2CO_{(g)} \quad \{\beta_2, \beta_3\} \tag{17}$$

$$H_{(a)} + H_{(a)} \rightarrow H_{2(g)} \quad \{\beta_2, \beta_3\} \tag{18}$$

$$H_{(a)} + CH_3O_{(a)} \rightarrow CH_3OH_{(g)} \quad \{\beta_2, \beta_3\} \tag{19}$$

$$\left.\begin{array}{ll} HC^{16}O^{18}O_{(a)} \rightarrow H_{(a)} + C^{16}O^{18}O_{(g)} & (20) \\ H_{(a)} + H_{(a)} \rightarrow H_{2(g)} & (21) \\ 2H_{(a)} + {}^{18}O_{(a)} \rightarrow H_2{}^{18}O_{(g)} & (22) \end{array}\right\}\{\gamma\}$$

The intermediate $H_2C^{16}O^{18}O$ was deduced on Cu(110) (*20*) and Ag(110) (*21*) during the oxidation of H_2CO on these surfaces. It was concluded from these studies that H_2CO was oxidized upon adsorption to $H_2C^{16}O^{18}O$ because only trace amounts of water were observed and while $H_2C^{16}O$ exchanged its oxygen-16 with surface oxygen-18 to form $H_2C^{18}O$. The H_2COO intermediate was not very stable on these surfaces and dissociated to $HC^{16}O^{18}O$ and hydrogen below 300°K. Since in that experiment H_2 evolution was desorption limited on copper, the exact temperature at which the formate was formed was not known. However, the presence of the $H_2(\beta_1)/CH_3OH$ peak suggested that $H_2C^{16}O^{18}O$ was present in this reaction because, had the formate been formed during the adsorption process, the hydrogen atoms would have been immediately oxidized to water. This experimental evidence supports the presence of a $H_2C^{16}O^{18}O$ intermediate on the Cu(110) surface during the oxidation of CH_3O,D but the exact steps by which this intermediate is produced from CH_3OD are still unclear.

The above mechanism includes three reaction pathways for the adsorption of methanol [steps (7), (8), and (11)]. Step (11) represents the nondissociative adsorption of CH_3OD whereas steps (7) and (8) represent the dissociative adsorption of CH_3OD. The nondissociative adsorption of methanol was probably due to stabilization of CH_3OH by the presence of other surface intermediates since very little methanol adsorbed on the oxygen-free Cu(110) surface. The data showed that all three pathways occurred in the oxidation of methanol on copper, but the final product distribution revealed that *methoxide was the most abundant surface intermediate.* The adsorption of CH_3OD at ~180°K resulted in the formation of four major distinct surface species: CH_3OD, CH_3O, $H_2C^{16}O^{18}O$, and water. Since below room temperature CH_3OD and water molecules desorbed, and $H_2C^{16}O^{18}O$ had released a hydrogen atom to form the formate only the intermediates CH_3O, $HC^{16}O^{18}O$, and H remained on the copper surface at room temperature.

The hydrogen atoms released when the intermediate $H_2C^{16}O^{18}O$ decomposed to $HC^{16}O^{18}O$, step (14), could either recombine and form H_2, step (15), or react with methoxide to form CH_3OH, step (16). The previous work with background D_2 (Fig. 2) clearly demonstrated that step (16) was fast above 300°K.

The formate, $HC^{16}O^{18}O$, was the most stable surface intermediate produced in this reaction and decomposed at 470°K to yield an adsorbed hydrogen atom and carbon dioxide, step (20). Some of the hydrogen atoms apparently reacted with residual surface oxygen atoms to form water, step (22), in addition to H_2, step (21). These oxygen atoms must have been strongly bound to the copper substrate because $H_2{}^{18}O$ was not observed at 365°K and higher temperatures were necessary to weaken this bond. The investigations of the decomposition of HCOOH and the oxidation of H_2CO on Cu(110) (*20*) revealed that, above 400°K formate was the only stable surface intermediate. Other investigators studying copper oxide catalysts utilized more complex molecules, i.e., propylene, and also observed the existence of formate intermediates (*22*). Summed up, these investigations suggest that formate was a very *stable* surface intermediate in the oxidation of hydrocarbons on copper.

Although the formate was the most *stable* intermediate, the methoxide was the most *abundant* intermediate on the partially oxidized Cu(110) surface. It was the *dissociation of the methoxide to formaldehyde and a hydrogen atom,* step (17), that *was responsible for the formation of formaldehyde from methanol.* The methoxide intermediate was not previously identified in other investigations as the intermediate responsible for the production of formaldehyde during the oxidation of methanol on copper and silver catalysts (*1–5, 23–26*). The hydrogen atoms released in this step could either recombine to H_2, step (18), or react with another methoxide to form CH_3OH, step (19). The overall selectivity for the oxidation of CH_3OD on Cu(110) was determined by the competition between steps (7) and (8). The experimental results showed that the *selectivity* for the oxidation of CH_3OD to 80% H_2CO and 20% $C^{16}O^{18}O$ was determined by the nature of the surface intermediates formed. The predominant pathway for the oxidation of methanol on Cu(110) was through the methoxide intermediate. It is interesting to consider the binding of this intermediate to the surface.

The methoxide was most probably bound to the copper substrate via the oxygen in CH_3O because: (a) the hydroxyl end of the methanol molecule interacted with surface oxygen-18 during the adsorption process to yield $D_2{}^{18}O$; (b) the oxygen in the methanol possesses a lone pair of electrons to share with the copper surface; and (c) the oxidation of CH_3CH_2OD on Cu(110) (*27*) exhibited the same chemistry as CH_3OD, which is consistent with both alkoxides bonding to the substrate via their oxygen. Fisher *et al.* concluded from angle-integrated ultraviolet photoemission that methanol bonding to Ru(110) substrate occurs via oxygen-derived orbitals (*28*). In other ultraviolet photoelectron spectroscopy (UPS) studies of CH_3OH adsorbed on other surfaces at low temperatures [ZnO(1$\bar{1}$00), polycrystalline Pd, and Ni(111)], the molecule was weakly perturbed by adsorption, and the effect on its molecular orbitals has been used to suggest that it is oriented with the oxygen nearer the surface (*29–31*). If the above conclusion is valid, then the frequency factor of $5.2 \pm 1.6 \times 10^{12}$ s^{-1} for the dissociation of $CH_3O_{(a)}$ to $H_2CO_{(g)}$ and $H_{(a)}$ appears to be a reasonable value for breaking the H–C bond through a cyclic intermediate.

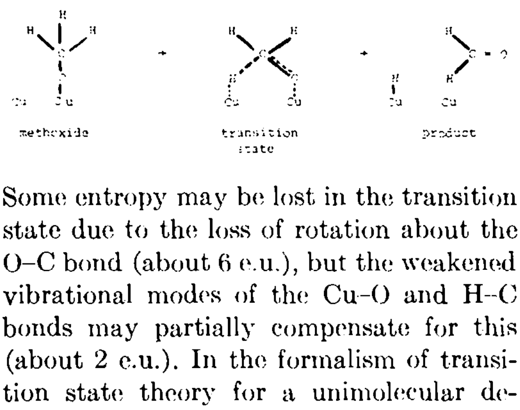

Some entropy may be lost in the transition state due to the loss of rotation about the O–C bond (about 6 e.u.), but the weakened vibrational modes of the Cu–O and H–C bonds may partially compensate for this (about 2 e.u.). In the formalism of transition state theory for a unimolecular decomposition (*32*),

$$\nu \approx 10^{13} \exp\left(\frac{\Delta S\ddagger}{R}\right) s^{-1}, \qquad (23)$$

where $\Delta S\ddagger$ is the entropy of activation and R is the gas constant. For the transition state depicted above, $\Delta S\ddagger \approx -4$ cal/gmole – °K, and $\nu \approx 10^{12}$ s^{-1}. The accuracy of our experimental numbers do not allow any further conclusions to be made, but a frequency factor of $5.2 \pm 1.6 \times 10^{12}$ s^{-1} seems reasonable for this step.

It is not known whether only one or both oxygens in $HC^{16}O^{18}O$ participated in bonding of the formate to the surface, but it is generally agreed that there does not exist a metal–carbon bond. Infrared studies of olefin adsorption on oxide surfaces have generally not indicated the presence of a metal–carbon bond and it was concluded that the organic fragment was held on the surface by a carbon–oxygen bond (*33*). Further evidence for the lack of a metal–carbon bond is suggested by the present observations that both methanol and formaldehyde reacted with *surface* oxygen-18 atoms to form $HC^{16}O^{18}O$ on Cu(110). Regardless of whether one or both oxygen atoms were bound to the copper substrate the frequency factor measured for the decomposition of $HC^{16}O^{18}O$ to carbon dioxide and hydrogen, $8 \pm 2 \times 10^{13}$ s^{-1}, also appeared to be a consistent value for breaking the H–C bond. In this respect the class of gas-phase reactions similar to breaking the H–C bond of *surface intermediates*, as postulated for the decomposition of CH_3O and $HC^{16}O^{18}O$ on a copper surface, are complex fission reactions with four- or five-center cyclic transition states (*34*). Table 3.5 of Ref. (*34*) lists many four-center complex fission reactions, and all have preexponential factors between 10^{13} and 10^{14} s^{-1}. Five-center complex fission reactions are listed in Table 3.7 of Ref. (*34*) and exhibit preexponential factors which may be one or two orders of magnitude less than 10^{13} s^{-1}. In general the frequency factors for a gas-phase fission reactions involving cyclic transition states are $\sim 10^{11}$–10^{14} s^{-1} and are in agreement with the preexponential factors observed for breaking the H–C bonds of CH_3O and $HC^{16}O^{18}O$ on Cu (110).

b. *The Effect of Adsorbed Oxygen*

The oxygen variation studies (Fig. 9) demonstrated that the amount of methanol

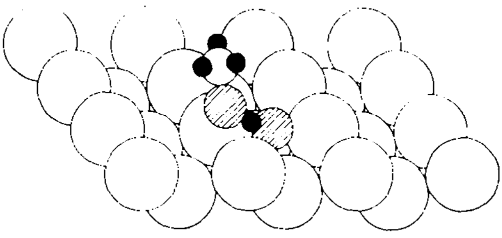

FIG. 10. A schematic representation for the adsorption of CH_3OH on a partially oxidized copper(110) surface. The oxygen covalent radius was used to represent the diameter of the adsorbed oxygen atom. Small filled circle = hydrogen atom; small empty circle = carbon atom; hatched circle = oxygen atom; large empty circle = copper atom.

adsorbed on the partially oxidized Cu(110) surface exhibited a maximum at approximately 20% surface coverage by adsorbed oxygen. Moreover the dissociative chemisorption of CH_2OH on copper was greatly enhanced through a highly specific interaction involving the hydroxyl end of the methanol molecule and a surface oxygen atom. This observation implies that zerovalent copper was not active for alcohol adsorption. The insertion of oxygen into the surface may create copper sites with a positive valence promoting adsorption of CH_3OD via interaction of the electron-donating oxygen lone pair. Furthermore, the $Cu^{\delta+}O^{\delta-}$ site may produce more efficient splitting of the O–D bond in CH_3OD. Such an interaction may require a specific geometric orientation of CH_3OD relative to the site, as shown schematically in Fig. 15, which may be quite sensitive to surface structure.

The oxidation of copper was studied under UHV conditions by low-energy electron diffraction (LEED) and ultraviolet photoelectron spectroscopy (UPS). Ertl (*35*) and Simmons *et al.* (*36*) examined the oxidation of Cu(110) by LEED and independently observed the formation of streaks in the diffraction pattern during the early stages of oxygen adsorption. These streaks were interpreted to be caused by oxygen initially adsorbed in the troughs of the (110) surface, as depicted in Fig. 10. Additional oxygen adsorption produced a (2 × 1) LEED pattern which was attributed to surface restructuring. Ertl observed the onset of the formation of the (2 × 1) LEED pattern at approximately 1 Langmuir of exposure of oxygen. The UPS spectra of the oxidation of Cu(110) have not been examined, but the results for the adsorption of oxygen on polycrystalline copper surfaces have been reported in the literature (*37, 38*). The UPS spectra of the initial adsorption of oxygen on the polycrystalline copper surfaces did not exhibit unusual characteristics that could account for the maximum in the methanol sticking probability as a function of oxygen exposure. The above results suggests that restructuring of the Cu(110) oxygen surface was probably responsible for the maximum in the sticking probability of methanol on Cu(110) as a function of oxygen exposure. This effect may be due to a decrease in the affinity of the copper for the methanol oxygen as the copper atom is surrounded by adsorbed oxygen.

The relative importance of the oxidation step,

$$CH_3OH_{(g)} + O_{(a)} \rightarrow H_2CO_{(g)} + H_2O_{(g)}, \quad (24)$$

versus the dehydrogenation step,

$$CH_3OH_{(g)} \rightarrow H_2CO_{(g)} + 2H_{(a)}, \quad (25)$$

$$H_{(a)} + H_{(a)} \rightarrow H_{2(g)}, \quad (26)$$

$$2H_{(a)} + O_{(a)} \rightarrow H_2O_{(g)}, \quad (27)$$

in the production of formaldehyde from methanol on copper and silver catalysts, has not been resolved previously. Thermodynamic calculations on the equilibrium relations for the dehydrogenation of methanol to formaldehyde showed that at atmospheric pressure the equilibrium conversions would be about 50% at 400°C, 90% at 500°C, and 99% at 700°C (*39*). Several investigators examined the production of formaldehyde from methanol in the absence of oxygen and found low conversions (*23, 24*) or almost no formaldehyde in the product gases (*7, 25*). The conversions predicted by thermodynamics were not observed experimentally. These results suggested that dehydrogenation was not the principle reaction, but some confusion still persisted because more formaldehyde was produced than could be accounted for by Eq. (24), based on the oxygen consumed, and a large amount of hydrogen was produced under oxidizing conditions. The mechanism proposed in the present study for the oxidation of methanol to formaldehyde readily accounts for these discrepancies:

$$CH_3OH_{(g)} + O_{(a)} \rightarrow CH_3O_{(a)} + OH_{(a)}, \quad (28)$$

$$CH_3OH_{(g)} + OH_{(a)} \rightarrow CH_3O_{(a)} + H_2O_{(g)}, \quad (29)$$

$$2CH_3O_{(a)} \rightarrow 2H_2CO_{(g)} + 2H_{(a)}, \quad (30)$$

$$H_{(a)} + H_{(a)} \rightarrow H_{2(g)}. \quad (31)$$

The above mechanism shows that it was only necessary for oxygen to react with the methanol hydroxyl hydrogen and that less oxygen was actually necessary than predicted by Eq. (24). The resultant overall reaction is

$$2CH_3OH + \tfrac{1}{2}O_2 \rightarrow 2H_2CO + H_2 + H_2O. \quad (32)$$

This mechanism also explains why the product gases contained significant amounts of hydrogen. Some of the hydrogen formed in step (30) was undoubtedly oxidized to water, but since the commercial process employs a rich mixture of methanol with air a substantial percentage of the hydrogen is not converted to water.

5. CONCLUSIONS

The results of this study clearly indicated that the active state of the copper surface for the oxidation of methanol was a partially oxidized surface. The oxygen activated the surface for methanol adsorption and removed the hydrogen released by water formation on the surface via a low-energy reaction pathway. In the oxidation several intermediates were identified. Adsorbed CH_3O was the dominant intermediate, and the oxidation selectivity was determined by the competitive formation of HCOO. The values of the preexponential factors observed for the elementary steps were consistent with the formation of cyclic transition states. This work illustrates further the applicability of UHV kinetic studies to more complex reaction systems.

APPENDIX I

THE EFFECT OF SURFACE OXYGEN CONCENTRATION ON ADSORPTION/DESORPTION AND SURFACE REACTION

The influence of oxygen upon the CH_3OH desorption spectra is presented in Figs. 11 and 12. Very little methanol adsorbed on the oxygen-free copper surface (Fig. 11a), but the methanol coverages increased substantially when the copper surface was predosed with oxygen. The surface concentration of oxygen not only determined the amount of CH_3OH adsorbed on the copper

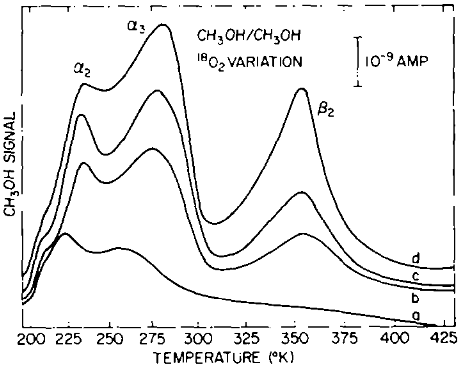

FIG. 11. The influence of low exposures of oxygen upon the CH_3OH desorption spectrum. The Cu(110) surface was oxidized at 295 ± 10°K and was given a 100-s dose of CH_3OH at 180°K. The oxygen exposures were (a) 0, (b) 0.3, (c) 0.5, and (d) 1 Langmuir.

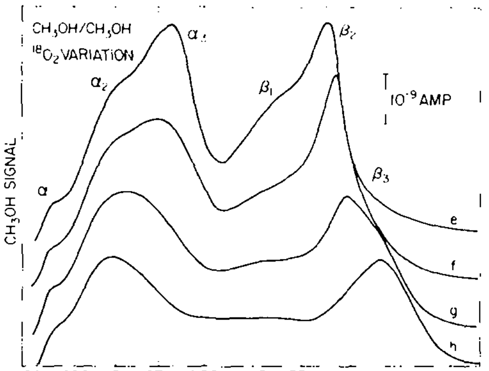

FIG. 12. The influence of high exposures of oxygen upon the CH_3OH desorption spectrum. The Cu(110) surface was oxidized at 295 ± 10°K and was given a 100-s dose of CH_3OH at 180°K. The oxygen exposures were (e) 2, (f) 3, (g) 5, and (h) 10 Langmuirs.

surface, but also altered the relative populations of the various methanol desorption states. The relative population of the methanol peaks was constantly altered as the oxygen exposure was varied; this was most dramatic at the highest exposure of oxygen (Fig. 12h), where the β_2 state had completely disappeared and was replaced by a new β_3 peak. If the preexponential factor were assumed constant, such a shift in the CH_3OH peak could be brought about by an increase of 1.5 kcal/mole in the activation energy. Overall the effects of surface oxygen on CH_3OH/CH_3OH were to produce a maximum in the sticking probability and to increase the activation energy of the binding state.

The results of low exposures of oxygen (0–1 Langmuirs) upon the production of formaldehyde from methanol are presented in Fig. 13. Little formaldehyde was formed on the oxygen-free copper surface (Fig. 13a), but the formaldehyde signal increased over an order of magnitude with oxygen exposure. *It was therefore necessary to have oxygen on the copper surface in order to produce efficiently formaldehyde from methanol.*

The H_2CO spectra observed at higher exposures of oxygen (2–10 Langmuirs) is shown in Fig. 14. Exposures of oxygen greater than 2 Langmuirs decreased the overall production of formaldehyde and altered the relative formation of formaldehyde from the β_2 and β_3 states. At 10

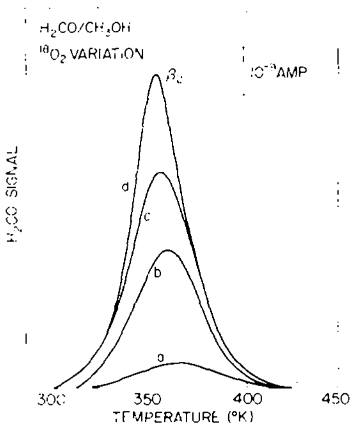

FIG. 13. The influence of low exposures of oxygen upon the H_2CO flash decomposition spectrum. The Cu(110) surface was oxidized at 295 ± 10°K and was given a 100-s dose of CH_3OH at 180°K. The oxygen exposures were (a) 0, (b) 0.25, (c) 0.5, and (d) 1.0 Langmuir.

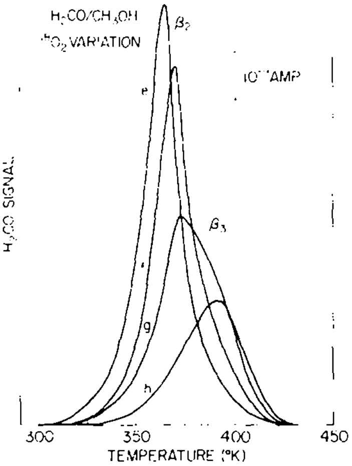

FIG. 14. The influence of high exposures of oxygen upon the H_2CO flash decomposition spectrum. The Cu(110) surface was oxidized at 295 ± 10°K and was given a 100-s dose of CH_3OH at 180°K. The oxygen exposures were (e) 2, (f) 3, (g) 5, and (h) 10 Langmuirs.

Langmuirs of exposure of $^{18}O_2$ (Fig. 14h), the β_2 peak was completely suppressed and only the β_3 peak was present. The symmetry of the $H_2CO(\beta_3)/CH_3OH$ peak indicated a first-order process and its kinetic parameters were therefore calculated by plotting the natural logarithm of rate divided by the coverage versus inverse surface temperature (*17*). The value found was

$$k_{H_2CO(\beta_3)/CH_3OH} = 1.5 \pm 0.7 \times 10^{10} \times \exp(-19.3 \pm 0.4\ \text{kcal/mole}/RT)\ \text{s}^{-1}. \tag{33}$$

The low preexponential factor and activation energy of $H_2CO(\beta_3)/CH_3OH$ may have been due to the broadening of curve h (Fig. 14) by the presence of some $H_2CO(\beta_2)/CH_3OH$. Such a broadening would prevent an accurate determination of the kinetic parameters. The similarities in the H_2CO and CH_3OH spectra above room temperature as a function of oxygen exposure in Figs. 11 to 14 again show that both products were related to the same surface intermediate.

The adsorption characteristics of CO, CO_2, and D_2 were compared on the clean and partially oxidized copper surfaces in order to understand better the influence of surface oxygen atoms upon the adsorption behavior of simpler molecules. The experiments were conducted by varying the oxygen exposure and subsequently exposing the partially oxidized surface to a constant amount of CO, CO_2, or D_2; the amount of gas exposed was always less than that necessary to produce saturation coverages. The results demonstrated that the ability of the copper surface to adsorb simple gases *decreased* with increasing oxygen coverage.

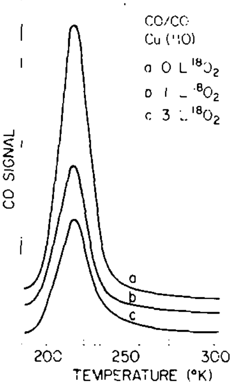

FIG. 15. The influence of surface oxygen upon the adsorption of carbon monoxide. The Cu(110) surface was oxidized at 295 ± 10°K and CO was adsorbed at 180°K.

The influence of surface oxygen upon the adsorption/desorption behavior of CO is presented in Fig. 15. The total amount of CO adsorbed decreased with initial exposure to oxygen, but the peak position appeared unaffected by the presence of surface oxygen. The adsorption of CO_2 also exhibited similar behavior. On the oxygen-free copper surface greater than 99% of the adsorbed CO_2 molecules dissociated to CO and surface oxygen. The magnitude of the CO/CO_2 peak was greatly diminished when the copper surface was predosed with 1 to 3 Langmuirs of oxygen. D_2 did not adsorb on either the clean or the partially oxidized surface (as reflected by the absence of D_2 and $D_2{}^{18}O$ signals).

These results demonstrated that the presence of oxygen atoms on the copper surface diminished the sticking probabilities of CO and CO_2; the lower sticking probabilities may be reflecting the decreased number of adsorption sites available to CO and CO_2. Furthermore, the oxygen variation results strongly suggest that the enhanced activity of the partially oxidized copper surface toward the adsorption of methanol was due to a highly specific interaction of the alcohol with the surface oxygen atoms. Since no HD or D_2 was observed to desorb when CH_3OD was adsorbed, and all of the deuterium atoms were reacted to $D_2{}^{18}O$ and $HD^{18}O$, the hydroxyl end of the methanol molecule must have interacted with the surface oxygen during the adsorption process.

TABLE 4

The Mass Spectrum of CH_3OH and CH_3OD[a]

m/e	CH_3OH		m/e	CH_3OD	
	Identity	Abundance		Identity	Abundance
31	CH_2OH	100	32	CH_2OD	100
32	CH_3OH	80	33	CH_3OD	79
29	CHO	33	29	CHO	18
15	CH_3	10	15	CH_3	10

[a] Data from Ref. (*40*).

APPENDIX II

Analysis of Mass Spectral Data

The various species that desorbed from the partially oxidized Cu(110) surface following adsorption of CH_3OD were readily identified by mass spectrometry. The major ionization peaks of CH_3OH ($M = 32$) and CH_3OD ($M = 33$) in the mass spectrometer are presented in Table 4 (*40*). The CH_3OH molecule gives rise to large $m/e = 31$, 32, 29, and 15 signals and the CH_3OD molecule gives rise to large $m/e = 32$, 33, 29, and 15 signals. The two forms of methanol are thus distinguishable by monitoring $m/e = 33$ for CH_3OD and $m/e = 31$ for CH_3OH. The $m/e = 33$, 32, and 31 signals were recorded subsequent to the adsorption of CH_3OD on a partially oxidized Cu(110) surface and are shown in Fig. 16. Only the $m/e = 33$ and 32 signals appeared below 300°K and they originated from CH_3OD; only the $m/e = 32$ and 31 signals appeared above 300°K and they originated from CH_3OH. Thus CH_3OH was monitored by recording the $m/e = 31$ signal and CH_3OD was recorded by monitoring the $m/e = 33$ signal.

The product $H_2C^{18}O$ ($M = 32$) was isolated in the oxidation of $H_2C^{16}O$ on Cu (110) (*20*) and also gives rise to large $m/e = 31$ and 32 signals (*41*). $H_2C^{18}O$ can be distinguished from CH_3OH by monitoring the $m/e = 15$ signal because formaldehyde does not have a CH_3 group. The $m/e = 15$ signal was monitored subsequent to the adsorption of CH_3OH on a partially oxidized surface and is shown in Fig. 17. Since a large $m/e = 15$ signal was observed above room temperature $H_2C^{18}O$

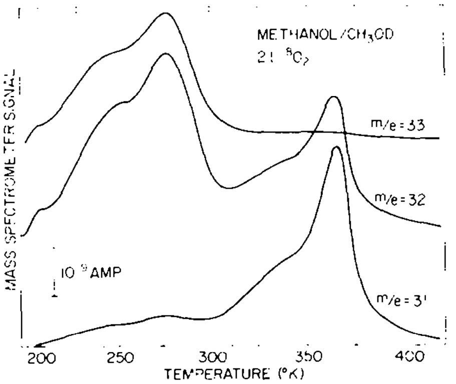

FIG. 16. The $m/e = 33$, 32, and 31 signals subsequent to the adsorption of CH_3OD at 180°K on a Cu(110) surface that was predosed with 2 Langmuirs of $^{18}O_2$ at 295 ± 10°K.

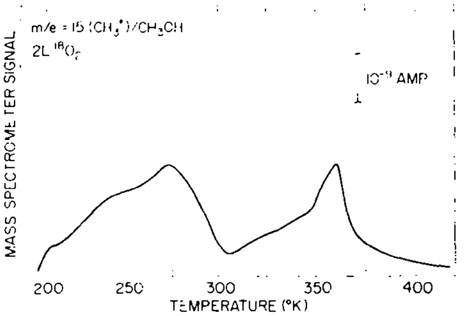

FIG. 17. The $m/e = 15$ (CH_3^+) signal following adsorption of CH_3OH at 180°K on a Cu(110) surface that was preoxidized at 295 ± 10°K with 2 Langmuirs of $^{18}O_2$.

was not a significant product in this reaction. Formaldehyde, H_2CO ($M = 30$), that resulted from the oxidation of methanol on Cu(110) was monitored by recording the $m/e = 30$ signal because neither CH_3OH or CH_3OD gave rise to substantial $m/e = 30$ signal.

The various isotopes of water observed below room temperature when CH_3OD was employed were monitored by recording the $m/e = 22$ ($D_2{}^{18}O$), the $m/e = 21$ ($HD^{18}O$), and the $m/e = 20$ ($H_2{}^{18}O$) signals. The $H_2{}^{18}O$ signal was corrected for $^{18}OD^+$ contributions from $D_2{}^{18}O$ and $HD^{18}O$ (*41*). The isotopes of carbon dioxide did not give rise to overlapping signals and were identified by recording the $m/e = 48$ ($C^{18}O^{18}O$), $m/e = 46$ ($C^{16}O^{18}O$), and $m/e = 44$ ($C^{16}O^{16}O$) signals.

ACKNOWLEDGMENT

The authors gratefully acknowledge the support of the National Science Foundation (NSF-ENG-74-15509) throughout the course of this work.

REFERENCES

1. Dixon, J. K., and Longfield, J. E., *in* "Catalysis" (P. H. Emmet, Ed.), Vol. 7, pp. 231–236. Reinhold, New York, 1960.

2. Walker, J. F., "Formaldehyde," pp. 1–36. Reinhold, New York, 1964.

3. Hader, R. N., Wallace, R. D., and McKinney, R. W., *Ind. Eng. Chem.* **44**, 1508 (1952).

4. Sabatier, P., and Mailhe, A., *Ann. Chim. Phys.* **8**, 20, 344 (1910).

5. Thomas, M. D., *J. Amer. Chem. Soc.* **42**, 867 (1920).

6. Lawson, A., and Thomson, S. J., *J. Chem. Soc. London* **2**, 1861 (1964).

7. Le Blanc, M., and Plaschke, E., *Z. Elektrochem.* **17**, 45 (1911).

8. Constable, F. H., *Proc. Roy. Soc. A* **107**, 270 (1925); Palmer, W. G., and Constable, F. H., *Proc. Roy. Soc. A* **107**, 255 (1925).

9. Frolich, P. K., Fenske, M. R., and Quiggle, A. M., *J. Amer. Chem. Soc.* **51**, 61 (1929); Frolich, P. K., Fenske, M. R., Perry, L. R., and Hurdy, N. L., *J. Amer. Chem. Soc.* **51**, 187 (1929).

10. K. Kawamoto, *Bull. Chem. Soc. Japan* **34**, 795 (1961).

11. J. C. Ghosh and K. M. Chakravarty, *J. Indian Chem. Soc.* **2**, 142 (1925); J. C. Ghosh and J. B. Bakshi, *J. Indian Chem. Soc.* **3**, 415 (1926); J. C. Ghosh and J. B. Bakshi, *J. Indian Chem. Soc.* **6**, 749 (1929).

12. McCarty, J., Falconer, J., and Madix, R. J., *J. Catal.* **30**, 235 (1973).

13. Yaws, C. R., and Hopper, J. R., *Chem. Eng.* **83**, 119 (1976).

14. Johnson, S. W., and Madix, R. J., *Surface Sci.* **66**, 189 (1977).

15. Davis, L. E., MacDonald, N. C., Palmberg, P. W., Riach, G. E., and Weber, R. E., "Handbook of Auger Electron Spectroscopy," pp. 1–18. Physical Electronics Industries, Inc., Edina, Minn., 1976.

16. McCarty, J., and Madix, R. J., *J. Catal.* **38**, 402 (1975).

17. Ying, D. H. S., Ph. D. dissertation, Stanford University, 1977.

18. Falconer, J., and Madix, R. J., *Surface Sci.* **48**, 393 (1975).

19. Falconer, J., Ph. D. dissertation, Stanford University, 1974.

20. Wachs, I. E., Ying, D. H. S., and Madix, R. J., to be published.

21. Wachs, I. E., and Madix, R. J., Unpublished results.

22. Gerei, S. V., Rozhkova, E. V., and Gorokhovatskii, Ya. B., *Dokl. Akad. Nauk SSSR* **201**, 379 (1970).

23. Planovskaya, I. P., and Topchieva, K. V., *Kinet. Catal.* **2**, 375 (1961).

24. Atroshchenko, V. I., and Kushnarenko, I. P., *Int. Chem. Eng.* **4**, 581 (1964).

25. Bhattacharyya, S. K., Nag, N. K., and Ganguly, N. D., *J. Catal.* **23**, 158 (1971).

26. Robb, D. A., and Harriott, P., *J. Catal.* **35**, 176 (1974).

27. Wachs, I. E., and Madix, R. J., to be published.

28. Fisher, G. B., Madey, T. E., Waclawski, B. J., and Yates, J. T., Jr., Proceedings, 7th International Vacuum Science Congress and 3rd International Conference on Solid Surfaces, Vienna, 1977.

29. Rubloff, G. W., Luth, H., and Grobman, W. D., *Chem. Phys. Lett.* **39**, 493 (1976).

30. Luth, H., Rubloff, G. W., and Grobman, W. D., *Surface Sci.* **63**, 325 (1977).

31. Rubloff, G. W., and Demuth, J. E., *J. Vac. Sci. Technol.* **14**, 419 (1977).

32. Boudart, M., "Kinetics of Chemical Processes," pp. 41–50. Prentice-Hall, Englewood Cliffs, N. J., 1968.

33. Sachtler, W. M. H., *Catal. Rev.* **4**, 27 (1970).

34. Benson, J. W., "Thermochemical Kinetics," pp. 75–82. Wiley, New York, 1968.

35. Ertl, G., *Surface Sci.* **6**, 208 (1967).

36. Simmons, G. W., Mitchell, D. F., and Lawless, K. R., *Surface Sci.* **8**, 130 (1967).

37. Wagner, L. F., and Spicer, W. E., *Surface Sci.* **46**, 301 (1974). Yu, K. Y., Spicer, W. E., Lindau, I., Pianetta, P., and Lin, S. F., *Surface Sci.* **57**, 157 (1976).

38. Evans, S., *Faraday Trans. 2 Chem. Phys.* **71**, 1044 (1975).

39. Newton, R. H., and Dodge, B. F., *J. Amer. Chem. Soc.* **55**, 4747 (1933).

40. Beynon, J. H., Fontaine, A. E., A. E., and Lester, G. R., *J. Mass Spectrom. Ion Phys.* **1**, 1 (1968).

41. Stenhagen, E., Abrahamson, S., and McLafferty, F. W. (Eds.), "Atlas of Mass Spectral Data," Vol. 1. Interscience, New York, 1969.